Forest and non-forest mapping with envisat ASAR images

Ling, F ; Li, Z ; Chen, E ; Huang, Y ; Tian, X ; Schmullius, C ; Leiterer, Reik ; Reiche, J ; Santoro, M

Abstract: Envisat Advanced Synthetic Aperture Radar (ASAR) dual-polarization data are shown to be effective for regional forest monitoring. To this scope, an automatic SAR image preprocessing procedure was developed using SRTM DEM and Landsat TM image for geocoding in rugged terrain and smooth terrain areas, respectively. An object-oriented forest and non-forest classification method is then proposed based on the HH to HV intensity ratio and HV images of ASAR data at single acquisition in winter. The developed methods were applied to forest and non-forest mapping in Northeast China. The overall accuracy, the user's accuracy and the producer's accuracy of forest are 83.7%, 85.6% and 75.7% respectively. The results indicate that the proposed methods are promising for operational forest mapping at regional scale.

FOREST AND NON-FOREST MAPPING WITH ENVISAT ASAR IMAGES

F. Ling[(1)], Z. Li[(2)], E. Chen[(2)], Y. Huang[(1)], X. Tian[(2)], C. Schmullius[(3)], R. Leiterer [(3)], J. Reiche[(3)], M. Santoro[(4)]

[(1)] Key Laboratory of Spatial Data Mining & Information Sharing of Ministry of Education, Fuzhou University, Fuzhou, 350002, China
Email: lfl@fzu.edu.cn
[(2)] Institute of Forest Resources Information Techniques, Chinese Academy of Forestry, Beijing, 100091, China
Email: zengyuan.li@caf.ac.cn
[(3)] Department of Earth Observation, Friedrich-Schiller University Jena, Jena, 07745, Germany
Email: c.schmullius@uni-jena.de. reik.leiterer@geo.uzh.ch
[(4)] Gamma Remote Sensing, 3073 Gümligen, Switzerland
Email: santoro@gamma-rs.ch

ABSTRACT

Envisat Advanced Synthetic Aperture Radar (ASAR) dual-polarization data are shown to be effective for regional forest monitoring. To this scope, an automatic SAR image preprocessing procedure was developed using SRTM DEM and Landsat TM image for geocoding in rugged terrain and smooth terrain areas, respectively. An object-oriented forest and non-forest classification method is then proposed based on the HH to HV intensity ratio and HV images of ASAR data at single acquisition in winter. The developed methods were applied to forest and non-forest mapping in Northeast China. The overall accuracy, the user's accuracy and the producer's accuracy of forest are 83.7%, 85.6% and 75.7% respectively. The results indicate that the proposed methods are promising for operational forest mapping at regional scale.

Key words: Envisat ASAR, Forest mapping, Object-oriented classification, Northeast China

1. INTRODUCTION

Forests are a dominant biome of the Earth and have an important impact on its economic and environmental well-being. Because of the timely and continuous Eearth observation capability, remote sensing satellites are beneficial to the understanding of forest status. The usefulness of optical satellite remote sensing is limited under cloudy weather conditions and reduced solar illumination. SAR (synthetic aperture radar), instead, can ensure data acquisition thanks to the independence on weather conditions and sun angle [1].

Satellite SAR data have been used for forest mapping at regional scale in boreal forest [2-6], tropical forest [7], and globally [8]. For the monitoring of forest of Northeast China [9], proposed a forest growing stock volume estimation method based on European Remote Sensing ERS-1/2 tandem coherence and produced a forest growing stock volume map for Northeast China, using data acquired during 1995 and 1996.
The Envisat Advanced Synthetic Aperture Radar (ASAR), launched in 2002, has more advanced features than ERS-1 and ERS-2, such as multi-incidence angle and multi-polarization imaging capabilities. In particular, the Alternative Polarization (AP) mode can acquire data with two polarizations simultaneously (HH/VV, HH/HV or VV/VH).

The objective of this paper is to present a regional forest / non-forest mapping method based on Envisat ASAR Alternative Polarization mode data at single acquisition. The approach has been applied to produce a forest and non-forest map for Northeast China for 2005.

2. TEST SITE AND DATA

2.1 Geographic area

Northeast China, covers 1.26 million km^2, 13% of China's total acreage, and includes eastern Inner Mongolia Autonomous Region, the Heilongjiang province, the Jilin province and the Liaoning province. Climate is temperate monsoon, with winter lasting more than half a year and precipitation concentrated in summer. The main forest areas in Northeast China are in Daxinganling, Xiaoxinganling and Changbaishan. The growing stock volume of Northeast China accounts for 1/3 of China's total forest stock volume.

2.2 Reference data

For geocoding of the SAR data, 90 m Shuttle Radar Topography Mission (SRTM) Digital Elevation Model (DEM) resampled to 100 m was used.

For geocoding of the ASAR images in flat terrain areas and for validation of the mapping result, we used a Landsat TM dataset for 2005 and the derived land use map for Northeast China. This land use map, with 30 m spatial resolution, has 10 thematic classes - conifer

forest, broad leaf forest, mixed forest, shrub, agricultural field, high density grassland, grassland, water, urban and a class named other. To use this land use map to validate our result, we combined the three forest classes and shrub into forest and the remainder into non-forest. Validation based on the national forest inventory dataset of the Jilin province resulted in an accuracy of 83% in terms of forest and non-forest.

2.3 SAR data

More than 900 multi-temporal ASAR images acquired between July 2004 and March 2005 were available for this study. The data were acquired in the Alternating Polarization mode along descending orbits (10 a.m. Local time). All images were acquired at nominal incidence angle of 23° and with HH/HV polarization. The ground range spatial resolution of the images is approximately 30 m, whereas the data are provided with a sampling of 12.5 m.

3. DATA PREPROCESSING

Data preprocessing consisted of 1) calibration, 2) multi-looking, 3) speckle filtering, 4) ratio image computation, 5) geocoding and 6) radiometric terrain correction. The images were calibrated using the calibration constant supplied by the European Space Agency. To obtain the output pixel size set to 50 m, images were averaged with multi-looking factors of 4 and 4 in range and azimuth respectively.

3.1 Image filtering

Filtering for speckle noise is necessary to avoid errors during the image segmentation and classification step. To reduce speckle noise while preserving the spatial resolution, we used multi-channel filtering [10], which makes full use of the HH and HV information of the data. A Lee filter with 3×3 window was used to further reduce the speckle.

3.2 Ratio image

Although the polarimetric ratio image between two images acquired with different polarization is a useful feature for classification and can suppress topographic effects on the SAR backscatter, it is more sensitive to speckle noise than either of the single image used for ratio computation. Therefore, we computed the ratio using the average values within a spatial window

$$\hat{r} = \frac{\frac{1}{M}\sum_{i=1}^{M} I_{HH,i}}{\frac{1}{M}\sum_{i=1}^{M} I_{HV,i}} \qquad (1)$$

where $I_{HH,i}$ and $I_{HV,i}$ are the mean intensity values of HH and HV image in the estimation window with M pixels.

3.3 Geocoding

To geocode the SAR images a procedure based on a lookup table linking the radar and the map geometry was used [11]. The lookup table is generated from orbital information and the SRTM DEM. Such data is also used to produce a simulated SAR image, which helps to identify ground control point (GCPs) to quantify possible offsets between the true map geometry and the geometry described in the lookup table. GCPs Correlation match between the SAR imagery and the corresponding simulated SAR imagery serves to identify the offsets. The estimate of the offsets is then used to refine the lookup table which is finally used to resample the SAR imagery from slant range geometry to map geometry.

Fig.1 shows the procedure implemented for geocoding the Envisat ASAR images. First, the orbit data and SRTM DEM were used to create a simulated SAR image. Second, GCPs were selected by correlation match between SAR and simulated SAR images. Third, the correlation match result was evaluated. If the number of GCPs was less than 20 or standard deviation of the GCP fit was over 0.4 (fraction of a pixel), the Landsat TM image, instead of the simulated SAR image, was used to identify GCPs through correlation match again. Finally, a lookup table that provided the transfer function between the slant-range and map geometry was produced based on the bilinear fit of the offset estimates in correspondence of the GCPs. The geocoding was finally carried out with this lookup table. The accuracy of the geocoding was within one pixel. The whole processing was completely automated based on the Gamma software commands and Unix script language.

All SAR images were geocoded to the Albers Conical Equal Area coordinate system with an ellipsoid defined by WGS84. The central longitude is 130°E. The two parallel lines are 47°N and 25°N. The SAR images were geocoded to a pixel size of 50 m.

Fig.2 shows the geocoded color composite ASAR mosaic of Northeast China, with the backscattered intensity at HH-polarization in the red and the blue channel, and the backscattered intensity at HV-polarization in the green channel. Forests correspond to areas appearing in green. Conversely to other land surfaces in the study area characterized by surface scattering, forests are the only land cover with predominant volume scattering. The stronger HV backscattering coefficient in forests explains the green color for forests in Fig.2.

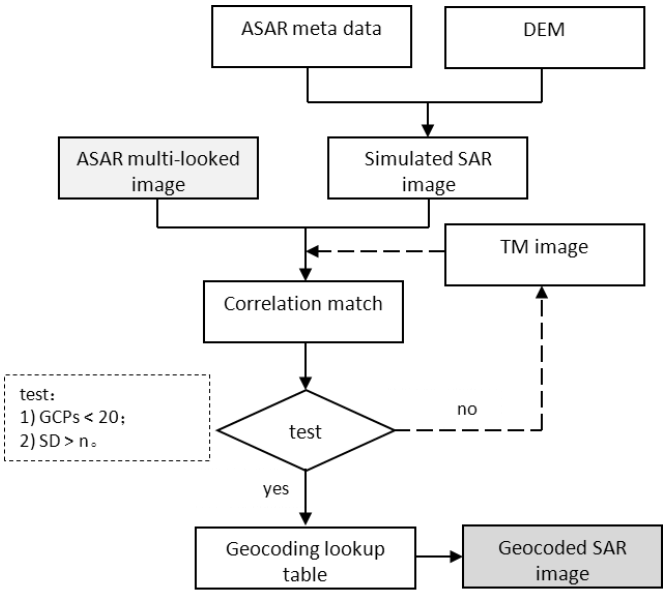

Figure 1. Flowchart of procedure implemented for geocoding of the Envisat ASAR images

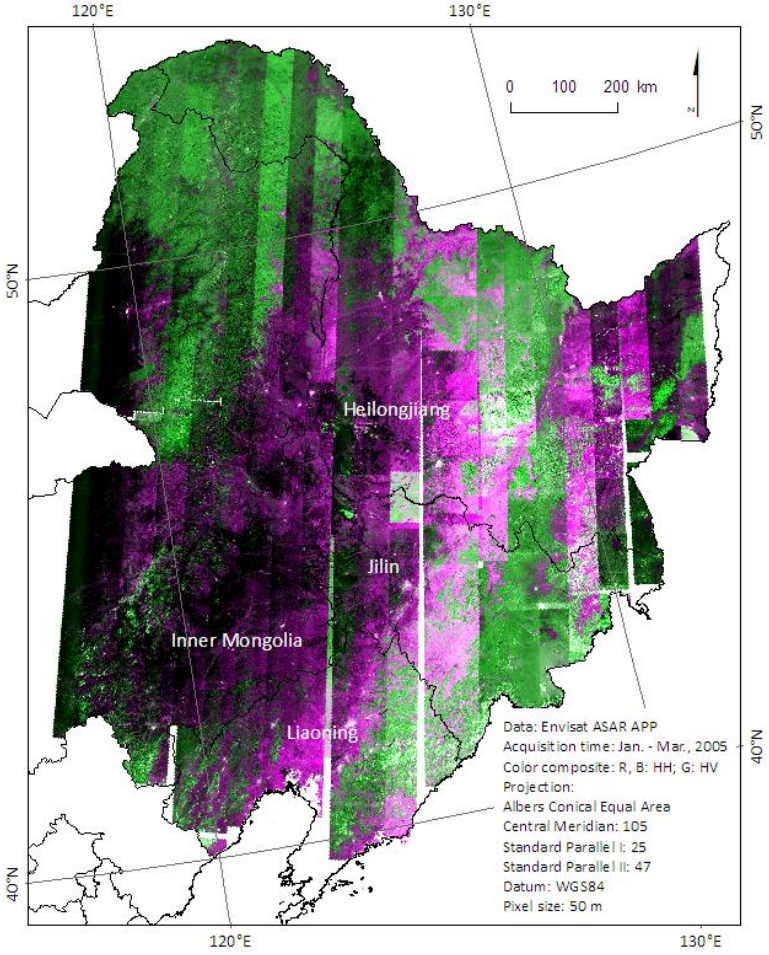

Figure 2. Envisat ASAR mosaic of Northeast China (color composite: R and B: backscattered intensity, HH-polarization; G: backscattered intensity HV-polarization)

4. FOREST / NON-FOREST CLASSIFICATION

The selection of data and data features is important to the classification accuracy. Therefore, we made analysis to determine the optimum SAR data acquisition time and the optimum data features as inputs for the classification algorithm. An object based hierarchical classification algorithm was then developed based on the analysis. eCognition software was used for the automation of the classification.

4.1 Data analysis

Image features, such as texture, polarimetric intensity ratio, geometric feature and relationship of the segmented image objects, can be derived from the original HH and HV images of Envisat ASAR data. The analysis was first performed by means of the eCognition software's Feature Space Optimization tool, which evaluated all the data features. The feature space optimization tool, together with visual comparison between different image features, showed that the polarimetric ratio between HH and HV intensity images was the best feature.

The Envisat ASAR data available can be divided to summer data (July 2004 - October 2004) and winter data (December 2004 - March 2005). Fig.3 shows the comparison of the histograms of example images for summer acquisition and winter acquisition. Fig.3 (a), (c) and (e) show that none of the summer HH, summer HV and summer ratio can separate forest from cropland. Fig.3 (f) shows that winter ratio is best for forest / non-forest discrimination. Water bodies, such as lakes and rivers, can also be separated from forest by the winter ratio image, although water bodies presented strong backscattering because of the increased surface roughness and volume scattering due to snow and ice cover.

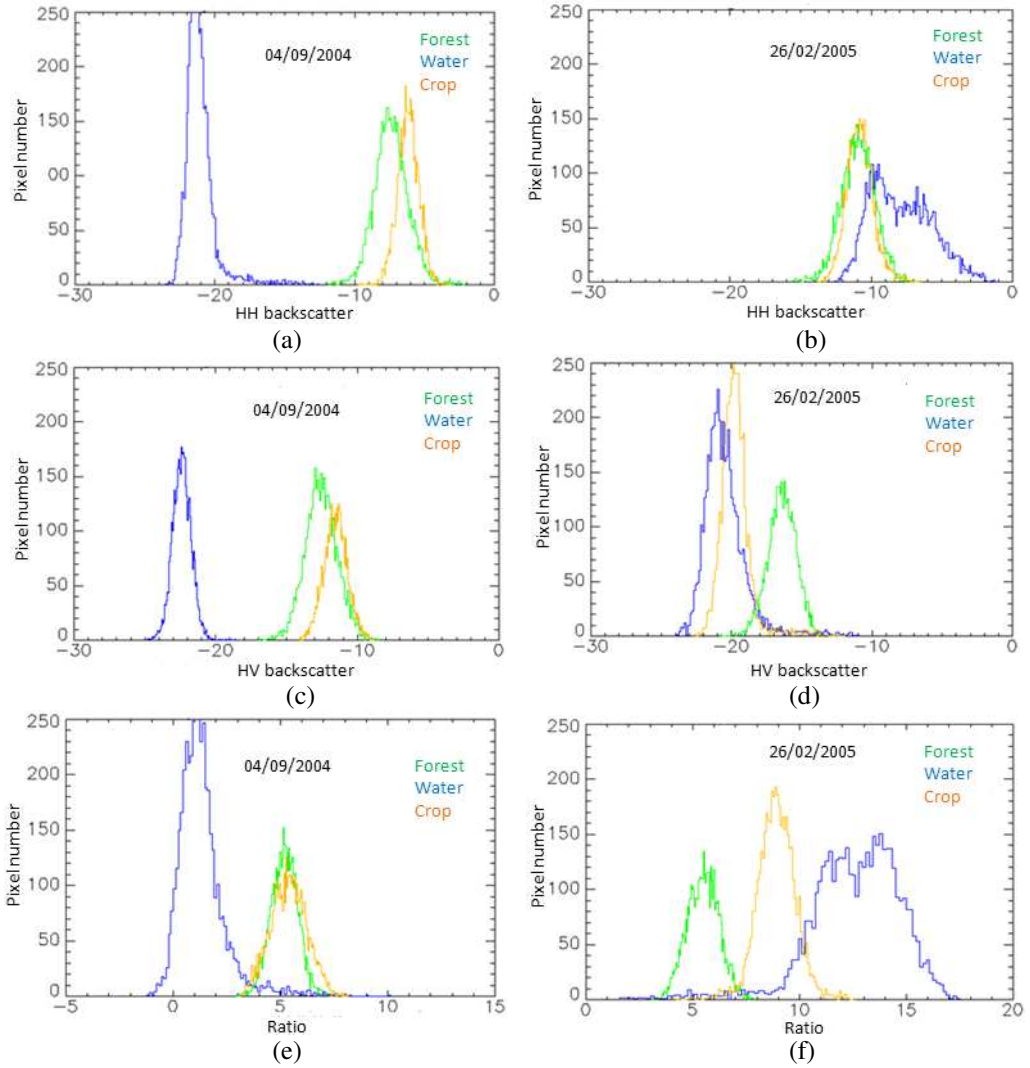

Figure 3. ASAR histograms of the typical land covers (left column(a),(c) and (e) are histograms of HH, HV and ratio image for summer data; right column (b),(d) and (f) are histograms of HH, HV and ratio image for winter data)

The histogram analysis show that winter data are more suitable for forest and non-forest classification than summer data, and that polarimetric intensity ratio is more suitable for forest / non-forest classification compared to HV-backscatter and HH-backscatter. In addition, we found that some vegetation types have similar low ratio values as that of forest, for example, the high density grassland in Inner Mongolia. However, this grassland vegetation has very low HV value, which is different from that of forest. Therefore, we used both polarimetric intensity ratio and the HV-backscatter image of the winter acquisitions (January 2005 - March 2005) as inputs for the following classification algorithm for forest and non-forest mapping in Northeast China.

4.2 Object oriented classification

Fig.4 shows the developed hierarchical classification method based on the ratio image and the HV-backscatter image of winter ASAR data. The eCognition-based method consists of image segmentation, object based classification and classification result optimization.

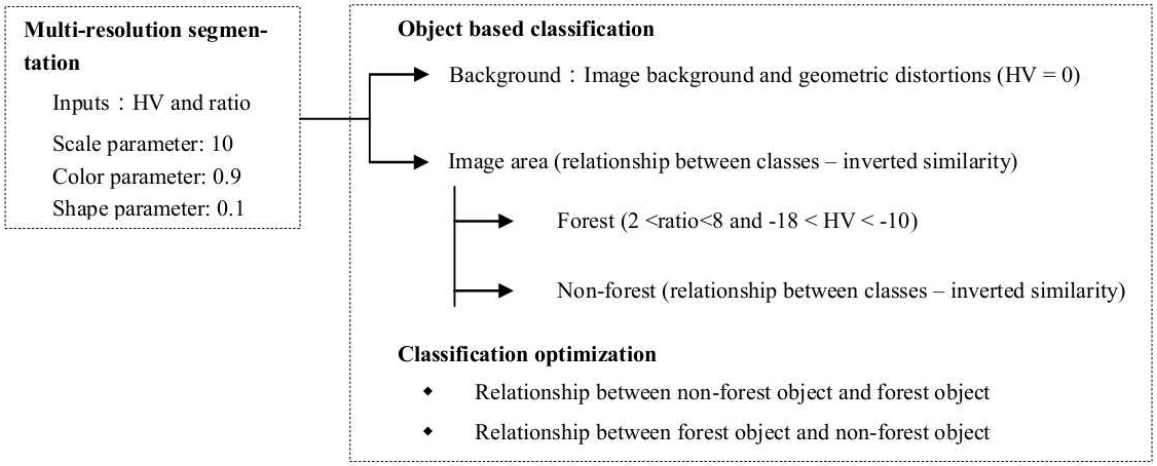

Figure 4. Flow chart of object based forest and non-forest classification using ENVISAT ASAR data

First, the multi-resolution segmentation method was used for image segmentation [12]. Three parameters determine the results of the multi-resolution segmentation: scale parameter, color parameter and shape parameter. The scale parameter determines the maximum allowed heterogeneity for the resulting image objects; the higher the value, the larger the resulting image objects. The object homogeneity to which the scale parameter refers is defined by the color parameter and the shape parameter. In most cases, the color criterion is the most important for creating meaningful objects, whereas the shape parameter can help to avoid highly fractured image object results in strongly textured data. Our goal is to make the segmented image objects as large and homogenous as possible. After trying different parameters, we used 10 as scale parameter, 0.9 as color parameter and 0.1 as shape parameter, mainly based on visual interpretation.

Then, a hierarchical classification was performed based on the segmented image objects. Object oriented classification can use not only the backscatter intensity information of the image but also the relationship between the objects. The first step of the classification with eCognition separated the image area from the background area using two rules: 1) HV mean object values equal to 0 for class Background and 2) the inverted similarity to Background objects was used for class Image area. The second step separated forest from non-forest within the Image area with the help of the class inheritance capability of eCognition. The dynamic ranges of ratio and HV intensity for forest were used to set the classification rules for class Forest; the inverted similarity to Forest was then used to classify Non-Forest objects. The thresholds shown in Fig.4 varied a little according to different strips at different acquisition time.

Finally, the relationship between the objects was used to optimize the initial classification. The initial classification included many small and discrete objects, for example, a forest object surrounded by continuous non-forest objects, or vice versa. The discrete classified objects were caused by two factors. One is the geometric and radiometric distortions due to topography in mountainous areas; the other is discretely distributed trees and other vegetation that have similar radar backscattering as that of forest. Two rules were set for the initial classification optimization: 1) reclassify a Non-Forest object to Forest when more than 80% of this Non-Forest object's border is adjacent to the borders of the surrounding Forest objects and 2) reclassify a Forest object to Non-Forest when more than 80% of this Forest object's border is adjacent to the borders of the surrounding Non-Forest objects. This optimization not

only made the classification map smoother than the initial by merging the small and discrete objects, but also classified the objects of foreshortening and layover. The automation of the classification process shown in Fig.4 was realized by eCognition's Processing Tree tool.

5. RESULT AND ERROR ANALYSIS

5.1 Classification result

Fig.5 shows the forest / non-forest map of Northeast China derived from Envisat ASAR winter data of 2005. Tab.1 shows the classification accuracy referring to the Landsat TM land use map. The accuracy measurement was based on the error matrix [13-14]. The Kappa coefficient is a measure for the reliability between the classification and the reference data, to estimate the random effect of the classification result. The overall accuracy is calculated by dividing the correctly classified pixels by the total number of pixels checked. The producer's accuracy is derived by dividing the number of correct pixels in one class divided by the total number of pixels as derived from reference data.

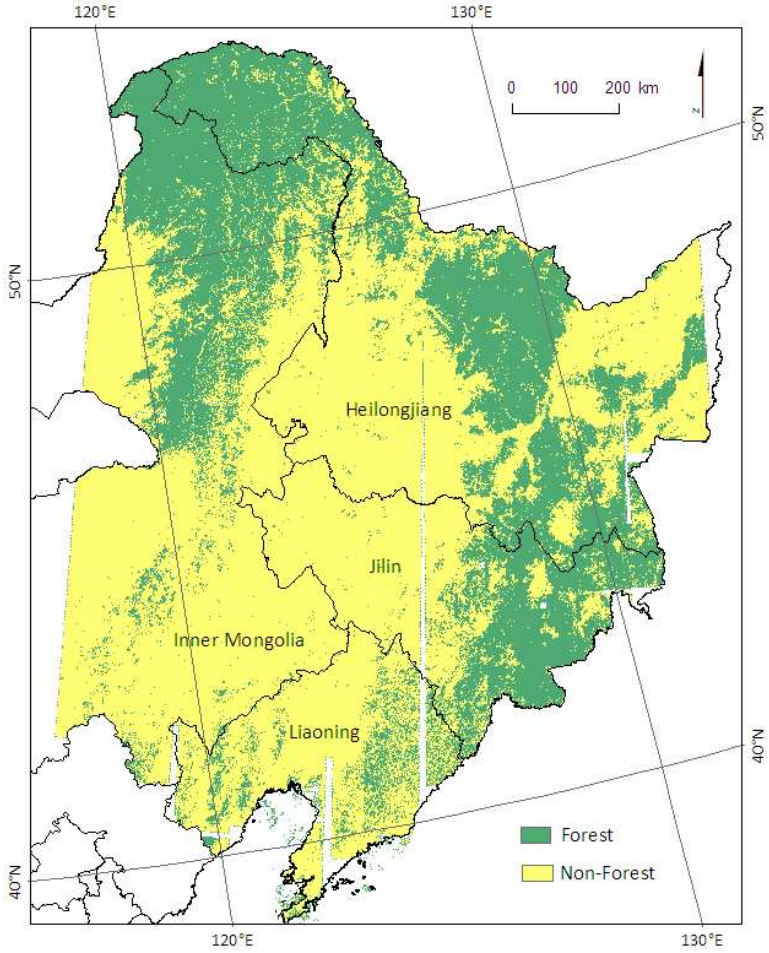

Figure 5. Forest and non-forest map of Northeast China from ENVISAT ASAR data

Table 1 Classification accuracy of forest and non-forest map of Northeast China

Kappa index	Overall accuracy	Forest user's accuracy	Forest producer's accuracy	Non-forest user's accuracy	Non-forest producer's accuracy
0.67	83.7%	85.6%	75.7%	82.6%	90%

5.2 Error analysis

Northeast China covers a large geographic area with various topography and different landscapes. The Envisat ASAR data were acquired at different time and under different meteorological conditions. The different environmental conditions under which the Envisat ASAR data were acquired complicated the use of one classification method to all the data. Fig.6 shows the classification error map based on the Landsat TM land use map. The commission error of the class "forest" was due to crop field and grassland. For example, the forest tree nursery, located in area A in Fig.6 in purple, was misclassified as forest due to similar backscattering.

Area B in Fig.6 shows another example of commission error for the class "forest" (the red area); this area was grassland in 2005 and recovered from a large forest fire that occurred in 2003. In some burned areas, however, some trees survived which implied that the area was misclassified as forest. Omission errors, i.e., forest areas misclassified as non-forest, were more significant than commission errors, as shown by the large blue area in Fig.6 and the low producer's accuracy of forest in Table 1. The omission of forest was primarily caused by terrain variations. The blue strips, along the azimuth direction in area C in Fig.6, show the problem of terrain variation and local incidence angle, causing the lower classification accuracy in the image near range than the accuracy in the far range. Omission of forest also occurred in area D and E, which are typical broken terrain with great variations.

The accuracy of the reference map used for validation should be considered for error analysis. Our field visit to Mohe county, in September 2011, confirmed that some areas labelled as grassland in the Landsat TM land use map were changed to forest in 2005; this indicates that the ASAR derived forest and non-forest map is correct in some areas, while the reference dataset presented some errors.

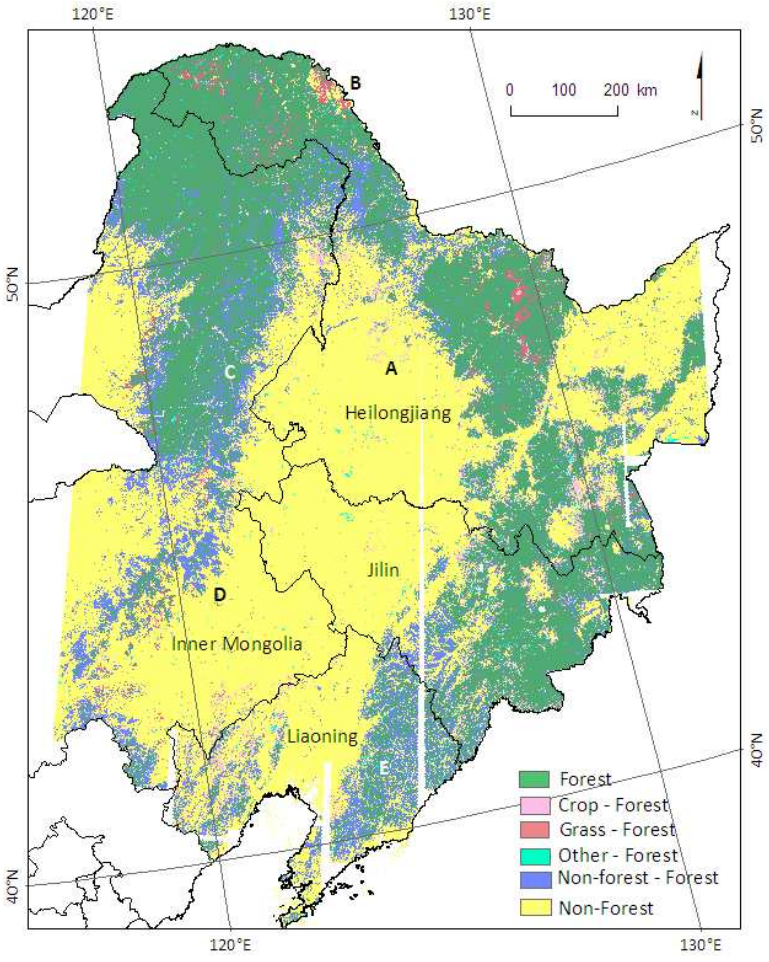

Figure 6. ASAR forest and non-forest classification error map

6. CONCLUSIONS

An automatic SAR data processing method and an object based forest and non-forest classification method were developed based on the ENVISAT ASAR HH/HV mode data. Satisfactory mapping accuracy was achieved when the methods were used for regional forest and non-forest mapping in Northeast China. The proposed methods are effective in timely and accurate regional forest and non-forest mapping.

7. ACKNOWLEDGEMENTS

The authors thank European Space Agency and the Ministry of Science and Technology of the P.R. China for supporting the work and Envisat ASAR data under Dragon Programme (ID:5314). This project is supported by the National Science Foundation for Young Scientists of China (Grant No. 41101381).

8. REFERENCES

1. Henderson, F.M. & Lewis, A.J. (1998). *Manual of Remote Sensing: Principles and Applications of Imaging Radar. Manual of Remote Sensing*, John Wiley & Sons Inc, New York, UK.
2. Schmullius, C., Holz, A. & Vietmeier, J.(1999). SIBERIA-results from the IGBP boreal forest transect. In *Geoscience and Remote Sensing Symposium. IGARSS'99 Proceedings. IEEE 1999 International*. pp 2118 –2120.
3. Baker, J., Balzter, H., Davidson, M., Eriksson, L., Gaveau, D., Gluck, M., Holz, A., Luckman, A., Marschalk, U., McCallum, I., Nilsson, S., Öskog, A., Quegan, S., Rauste, Y., Roth, A., Schmullius, C., Shvidenko, A., Tansey, K, Le Toan, T., Vietmeier, J., Wagner, W., Wegmüller, U., Wiesmann, A. & Yu, J. J. (2001). SAR Imaging For Boreal Ecology and Radar Interferometry – Final report. Online at *http://www.siberia1.uni-jena.de/* (as of 3 July, 2002).
4. Wagner, W., Luckman, A., Vietmeier, J., Tansey, K., Balzter, H., Schmullius, C., Davidson, M., Gaveau, D., Gluck, M., Le Toan, T., Quegan, S., Shvidenko, A., Wiesmann, A. & Yu, J.J.(2003). Large-scale mapping of boreal forest in SIBERIA using ERS tandem coherence and JERS backscatter data. Remote Sensing of Environment. 85(2), 125–144.
5. Rosenqvist, A., Shimada, M., Chapman, B., McDonald, K., De Grandi, G., Jonsson, H., Williams, C., Rauste, Y., Nilsson, M., Sango, D. & Matsumoto, M.(2004). An overview of the JERS-1 SAR Global Boreal Forest Mapping (GBFM) project. In *Geoscience and Remote Sensing Symposium, 2004. IGARSS '04. Proceedings. 2004 IEEE International*. pp 1033 – 1036.
6. Rauste, Y.(2005). Multi-temporal JERS SAR data in boreal forest biomass mapping. Remote Sensing of Environment. 97(2), 263–275.
7. Shimada, M., Isoguchi, O., Motooka, T., Shiraishi, T., Mukaida, A., Okumura, H., Otaki, T., Itoh, T., Rosenqvist, A., Kato, A. & Sasai, T.(2011). Generation of 10m resolution palsar and jers-sar mosaics and forest/non-forest maps for forest carbon monitoring. In *Geoscience and Remote Sensing Symposium (IGARSS), 2011 IEEE International.* pp 3510 –3513.
8. De Grandi, G., Mayaux, P., Rauste, Y., Rosenqvist, A., Simard, M. & Saatchi, S.S.(2000). The Global Rain Forest Mapping Project JERS-1 radar mosaic of tropical Africa: development and product characterization aspects. *IEEE Transactions on Geoscience and Remote Sensing*. 38(5), 2218 – 2233.
9. Cartus, O., Santoro, M., Schmullius, C. & Li, Z.(2011). Large area forest stem volume mapping in the boreal zone using synergy of ERS-1/2 tandem coherence and MODIS vegetation continuous fields. *Remote Sensing of Environment.* 115(3), 931–943.
10. Quegan, S. & Yu, J.J.(2001). Filtering of multichannel SAR images. *IEEE Transactions on Geoscience and Remote Sensing*. 39(11), 2373 – 2379.
11. Wegmuller, U.(1999). Automated terrain corrected SAR geocoding. In *Geoscience and Remote Sensing Symposium, 1999. IGARSS'99 Proceedings. IEEE 1999 International*. pp 1712 – 1714.
12. Benz, U.C., Hofmann, P., Willhauck, G., Lingenfelder, I. & Heynen, M.(2004). Multi-resolution, object-oriented fuzzy analysis of remote sensing data for GIS-ready information. *ISPRS Journal of Photogrammetry and Remote Sensing* 58(3-4), 239–258.
13. Congalton, R.G.(1991). A review of assessing the accuracy of classifications of remotely sensed data. *Remote Sensing of Environment*. 37(1), 35–46.
14. Foody, G.M.(2002). Status of land cover classification accuracy assessment. *Remote Sensing of Environment*. 80(1), 185–201.